Journal of Marine Systems 78 (2009) S244–S254

Contents lists available at ScienceDirect

Journal of Marine Systems

journal homepage: www.elsevier.com/locate/jmarsys

On the development and verification of a 2-D coupled wave-current model on unstructured meshes

Aron Roland [a,1], Andrea Cucco [b], Christian Ferrarin [c], Tai-Wen Hsu [d,*], Jian-Ming Liau [e,2], Shan-Hwei Ou [f], Georg Umgiesser [c], Ulrich Zanke [a]

[a] Institute for Hydraulic Engineering and Water Resources Management, Technische Universität Darmstadt, Rundeturmstr. 1, 60483 Darmstadt, Germany
[b] Institute for the Coastal Marine Environment, National Research Council, (IAMC-CNR), 09072, Torregrande, Oristano, Italy
[c] Institute of Marine Science, National Research Council (ISMAR-CNR), Castello 1364/b, 30122, Venice, Italy
[d] Department of Hydraulic and Ocean Engineering National Cheng Kung University 1 University Road, Tainan 701, Taiwan
[e] Taiwan Typhoon and Flood Research Institute, National Applied Research Laboratoriese
[f] Department of Environmental Resources Management, Tajen University, 20, Weishin Road, Yanpu Shiang, Pingtung, 907, Taiwan

ARTICLE INFO

Article history:
Received 18 December 2007
Received in revised form 2 December 2008
Accepted 22 January 2009
Available online 1 March 2009

Keywords:
Wave–current interactions
Spectral wave modelling
Shallow Water Equations
Unstructured meshes

ABSTRACT

In this paper, the numerical framework for a freely available fully coupled wave-current model, which solves the Shallow Water and the Wave Action Equation (WAE) on unstructured meshes in geographical space and some first applications are presented. It consists of the hydrodynamic model SHYFEM (Shallow Water Hydrodynamic Finite Elements Model), and the 3rd generation spectral wave model WWM (Wind Wave Model). The application of numerical schemes on unstructured meshes renders the coupled model more efficient in resolving the model domain, the bathymetry and the involved gradient fields of currents, water levels and wave action.

The source codes of the models have been coupled using FIFO (First In First Out pipes) data files. This technique makes an effective model coupling possible without cumbersome merging of both codes. Furthermore, it gives both source codes a universal interface for coupling with other flow or wave models. The coupled model was applied to simulate extreme events occurring in the Gulf of Mexico and the Adriatic Sea. In particular the wind and wave-induced storm surge generated by Hurricane Ivan was investigated and the results have been compared to the tidal gauge at Dauphin Island with reasonable results. For the case of the Adriatic Sea, the model, validated for the year 2004, has been applied to simulate waves and water levels induced by the century storm in November 1966 that lead to catastrophic and widespread damages in the regions of the Venice Lagoon. The obtained results have been compared to in situ measurements with respect to the wave heights and water level elevations revealing good accuracy of the model in reproduction of the investigated events. Especially, the Hurricane Ivan simulations showed the importance of inclusion of the wave–current interactions for the hindcast of the water levels during the storm surge. In a comparison to water level measurements at Dauphin Island, inclusion of the wave induced water level setup reduced the root mean square error from 0.13 to 0.11 m and increased the correlation coefficient from 0.75 to 0.79.

For the case of the Venice Lagoon, the comparison with the measurements showed that the model without wave–current interactions led to a good hindcast of water levels for the location Punta Salute, which is located in the inner part of the Lagoon. Nevertheless, the comparison of subsequent simulations with and without the influence of the waves clearly showed a simulated effect of intense wave setup-up in the coastal area in front of the lagoon, which is plausible given the intensity of flooding that occurred there.

1. Introduction

The simulation of the wave and current regime in complicated coastal environments is of great importance for coastal engineering practice or the effective planning of navy maneuvers and rapid environmental assessment. The application of freely available modelling systems that apply structured meshes for the discretization of the governing equation in geographical space is rather cumbersome in coastal regions with rapidly varying bathymetry and complicated

* Corresponding author. Tel.: +886 6 2757575ext63201, +886 6 2372315.
E-mail address: twhsu@mail.ncku.edu.tw (T.-W. Hsu).
[1] Tel.: +49 6151164843; fax: +49 6151163223.
[2] Taiwan Typhoon and Flood Research Institute, No.22, Keyuan Rd., Central Taiwan Science Park, Taichung City 40763, Taiwan.

0924-7963/$ – see front matter © 2009 Elsevier B.V. All rights reserved.
doi:10.1016/j.jmarsys.2009.01.026

current fields. In certain situations, complicated nesting strategies need to be undertaken in order to reproduce the wave height and current distribution accurately.

In many situations, waves and currents are strongly influenced by each other, because of their interactions. In order to simulate numerically the influence of the currents on the waves and vice versa, numerical wave models are coupled with currents models that solve the Shallow Water Equations. Actually, freely available 3rd generation spectral wave models exist that use structured meshes in geographical space to solve the Wave Action Equation (WAE). This can be efficient when considering open seas or coastal areas characterized by simple geometry, which can be easily discretized using structured meshes in geographical space. When wave–current interaction has to be investigated in complicated and heterogeneous environments, like lagoons or coastal seas, the use of numerical models that apply unstructured meshes is more efficient. Numerical models based on structured meshes cannot optimize the location of the grid points in order to solve the involved gradient field efficiently. Nested calculation, with fine grids in certain areas, sometimes must be carried out in order to have a proper representation of the different physical processes. Especially, when different classes of models are coupled with each other, like wave- and current- or even morphodynamic models, nesting procedures become complicated tasks. In these cases, the exchange of information between different models and different numerical grids may become cumbersome. With respect to the simulation of wind waves the application of unstructured meshes, rather than structured ones, must be seen especially in the context of a growing understanding of the nonlinear processes in deep and shallow water. The development of more sophisticated theories and algorithms to evaluate the nonlinear energy transfer, not only in homogenous (Hasselmann, 1962; Zakharov, 1968) but also in inhomogeneous media (e.g. Rasmussen, 1998; Stiassnie, 2001), results in more complicated formulae and numerical schemes. New developments in this context lead to more complicated theories and algorithms for the calculation of the nonlinear energy fluxes within the wave spectrum e.g. Webb–Resio–Tracy Method (e.g. van Vledder, 2006). These transfer integrals must be evaluated at every time step and grid point. Efficient discretization of the model domain using unstructured meshes reduces the computational demand for these source terms significantly and makes a more sophisticated model formulation possible (see, e.g., Ardhuin et al., 2007).

In this paper, we show the results of ongoing developments in order to provide an easy to use fully coupled wave–current model on unstructured meshes in geographical space for the research and engineering community. In particular, SHYFEM (Umgiesser et al., 2004), a hydrodynamic finite element model was coupled with a new version (WWM II; Roland, 2009) of the WWM (Hsu et al., 2005a).

In the first part of the paper, the governing equations of the current and wave model, and the implemented numerical schemes and the coupling procedure are summarized. In the second part, the performance of the coupled model was evaluated for the cases of the passage of Hurricane Ivan in the Gulf of Mexico, in the year 2004 and a strong Sirocco event in the Adriatic Sea, which occurred in 1966.

2. Governing equations and numerical schemes

2.1. The hydrodynamic model

The hydrodynamic model is a 3D finite element model developed at the ISMAR-CNR of Venice and successfully applied to several coastal environments (Ferrarin and Umgiesser, 2005; Umgiesser, 1997; Umgiesser and Bergamasco, 1995; Scroccaro et al., 2004).

In this study, the 2D version of the model code has been used. The model uses finite elements for the integration in geographical space and a semi-implicit algorithm for integration in time. The terms treated implicitly are the water level gradient and the Coriolis term in the momentum equation and the divergence term in the continuity equation. The friction term is treated fully implicitly; all other terms are treated explicitly.

The model solves the Shallow Water Equation in their formulations with water levels and transports, which in the 2D version reads as:

$$\frac{\partial U}{\partial t} - fV + gH\frac{\partial \zeta}{\partial x} + RU + X = \frac{F_x}{\rho H} \tag{1}$$

$$\frac{\partial V}{\partial t} + fU + gH\frac{\partial \zeta}{\partial y} + RV + Y = \frac{F_y}{\rho H} \tag{2}$$

$$\frac{\partial \zeta}{\partial t} + \frac{\partial U}{\partial x} + \frac{\partial V}{\partial y} = 0 \tag{3}$$

where ζ is the water level, U and V the vertically integrated velocities (total transports) in the x and y directions, g the gravitational acceleration, $H = h + \zeta$ the total water depth, h the undisturbed water depth, t the time, R the friction parameter and f is the Coriolis term.

The terms X and Y contain all other terms such as the wind stress, the nonlinear advective terms and those terms that need not be treated implicitly in the time discretization as they do not influence the model stability.

F_x and F_y represent the gradients of the radiation stress induced by waves (see Eqs. (14) and (15) in Section 2.3).The friction term is nonlinear and has been expressed as:

$$R = \frac{c_D}{H}\sqrt{u^2 + v^2} \tag{4}$$

with C_D is the bottom drag coefficient ($C_D = 0.0025$).

At the open boundary, the water levels are prescribed in accordance with the Dirichlet condition, while at the closed boundaries, only the normal velocity is set to zero and the tangential velocity is a free parameter. This corresponds to a full slip condition.

2.2. The wave model

The Wave Action Equation, describing growth, decay, advection and refraction of wind waves due to depths and currents (computed by the hydrodynamic model), can be written for Cartesian coordinates as follows:

$$\underbrace{\frac{\partial}{\partial t}N}_{\text{Change in time}} + \underbrace{\nabla_{\vec{x}} \cdot \left(c_{\vec{x}} N\right)}_{\text{Advection in geographical space}} + \underbrace{\frac{\partial}{\partial \sigma}(c_\sigma N) + \frac{\partial}{\partial \theta}(c_\theta N)}_{\text{Intra-spectral propagation}} = \underbrace{S_{tot}}_{\text{Total source term}} \tag{5}$$

where $N = N(t,x,y,\sigma,\theta)$ is the wave action density spectrum; t is the time; c_x and c_y are the wave propagation velocities in x and y space, respectively; c_σ and c_θ are the wave propagation velocities in σ and θ space, respectively; σ is the discrete relative frequency and θ is the wave propagation direction. The propagation velocities in the different phase spaces are given according the linear wave theory (e.g. Whitham, 1974) and can be written as:

$$\dot{\boldsymbol{X}} = \boldsymbol{c}_X = \frac{d\boldsymbol{X}}{dt} = \frac{\partial \sigma}{\partial k} + \boldsymbol{U} = \boldsymbol{c}_g + \boldsymbol{U} = \frac{1}{2} \cdot \left[1 + \frac{2kH}{\sinh(2kH)}\right] \cdot c_p = n \cdot c_p \tag{6}$$

$$\dot{\theta} = c_\theta = \frac{1}{k}\frac{\partial \sigma}{\partial H}\frac{\partial H}{\partial m} + \boldsymbol{k} \cdot \frac{\partial \boldsymbol{U}}{\partial s} \tag{7}$$

$$\dot{\sigma} = c_\sigma = \frac{\partial \sigma}{\partial H}\left(\frac{\partial H}{\partial t} + \boldsymbol{U} \cdot \nabla_{\boldsymbol{X}} H\right) - c_g \boldsymbol{k}\frac{\partial \boldsymbol{U}}{\partial s} \tag{8}$$

Here $\boldsymbol{U}$ is the mean velocity vector of the fluid; $\boldsymbol{k} = (k_x,k_y)$, $\boldsymbol{k}$ is the wavenumber vector and its absolute values respectively. $\boldsymbol{X} = (x_1,x_2)$ is the coordinate vector in geographical space, and s and m are unit vectors pointing in discrete direction θ_i and perpendicular to it, respectively. c_g is the wave-group velocity vector following from the linear theory with c_p, the wave phase velocity defined through the linear dispersion relation as:

$$c_p = \frac{\sigma}{k} = \sqrt{\frac{g}{k}\tanh(kH)} \tag{9}$$

The term S_{tot} at the right-hand side of Eq. (5) describes the net source terms defined by the energy input due to wind (S_{in}), the nonlinear interaction in deep and shallow water (S_{nl4} and S_{nl3}), the energy dissipation due to whitecapping and depth induced wave breaking (S_{ds} and S_{br}) and the energy dissipation due to bottom friction (S_{bf}).

$$S_{tot} = S_{in} + S_{nl4} + S_{ds} + S_{nl3} + S_{br} + S_{bf} \tag{10}$$

The nonlinear terms S_{nl4} and S_{nl3} have been evaluated in this study with the DIA (Discrete Interaction Approximation; Hasselmann and Hasselmann, 1985) and the Lumped Triad Approximation (LTA; Eldeberky, 1996) respectively. The WWM incorporates in addition the possibility to use the WRT (Webb–Resio–Tracy) method according to van Vledder (2006) or the MDIA (Multiple Discrete Interaction Approximation) by Hashimoto and Kawaguchi (2001). The dissipation formulation for bottom friction is based on the empirical JONSWAP formula (Hasselmann et al., 1973), which is parameterized as suggested by Bouws and Komen (1983) for Wind–Sea conditions. For the depth-induced wave breaking, the formulation of Battjes and Janssen (1978) was implemented. The WWM II incorporates the WAM Cycle 3 (Komen et al., 1984) and Cycle 4 (Günther et al., 1992) wind-input and white-capping dissipation formulations. The NEDWAM model physics according to Makin and Stam (2003) have been additionally incorporated into WWM II (Roland et al., 2005). Here the wind input function and the friction velocity are calculated on the foundation of the Wind Over Waves Coupling theory (WOWC; Makin and Kudryavtsev, 1999; Kudryavtsev et al., 1999). The white-capping dissipation function is defined according to Alves et al. (2002) and parameterized as suggested by Makin and Stam (2003). The NEDWAM model physics are used as a default formulation in the WWM since in preceding studies they showed improvements with respect to the hindcast of the spectral shape as well as the average period (Roland et al., 2005, 2006a,b).

The rather formidable task to solve the multidimensional problem of Eq. (5) was accomplished, as suggested, e.g., by Tolman (1995) or Hsu et al. (2005a), using the “Fractional Step method” of Yanenko (1971), by splitting the equation into the well-defined one and two-dimensional differential equations given below.

$$\frac{\partial N^{*}}{\partial t} + \frac{\partial}{\partial \theta}(c_\theta N) = 0; \left[N^{*}_{(t=0)} = N_0\right] \text{on } [0, \Delta t] \tag{11}$$

$$\frac{\partial N^{**}}{\partial t} + \frac{\partial}{\partial \sigma}\left(c_\sigma N^{*}\right) = 0; \left[N^{**}_{(t=0)} = N^{*}_{(t=\Delta t)}\right] \text{ on } [0, \Delta t] \tag{12}$$

$$\frac{\partial N^{***}}{\partial t} + \nabla_{\boldsymbol{x}}\left(\boldsymbol{c_x} N^{**}\right) = S_{(N^{**},),tot}; \left[N^{***}_{(t=0)} = N^{**}_{(t=\Delta t)}\right] \text{ on } [0, \Delta t] \tag{13}$$

For the solution of the WAE in directional space, Eq. (11), the original version of the WWM utilizes the Crank–Nicolson scheme, and for the solution of the WAE in geographical space, Eq. (13), the CNTG (Crank–Nicolson Taylor–Galerkin) FEM of Donea (1984) and Selmin et al. (1985) has been implemented into the WWM by Hsu et al. (2005a). The above-mentioned schemes are non-monotone and result in oscillations when strong gradients in the solution are present. In order to remedy this behaviour, alternative numerical schemes have been implemented into the WWM II.

For the integration of the WAE in spectral space, Eqs. (11) and (12), the Ultimate Quickest (UQ) scheme of Leonard (1991) was included in the new version of the WWM as suggested by Tolman (1995) and used in the WWIII model (Wave Watch III, Tolman, 2002). In order to solve Eqs. (11) and (12), the wave action spectrum is discretized in so-called spectral bins $\Delta\theta\Delta\sigma$. In the WWM, this is done with a constant directional distribution $\Delta\theta$ and a frequency distribution that is defined as a constant ratio $\Delta\sigma/\sigma$, which results in logarithmically distributed frequency increments. The logarithmic distribution in frequency space is chosen to efficiently resolve the steep gradients that are present in the low frequency part of the spectrum and it improves the accuracy of the DIA (see e.g. Tolman, 2002).

The UQ-scheme is an explicit third order space/time scheme, which is conservative and monotone for CFL (Courant–Friedrich–Levy) numbers smaller than unity. In the WWM II, linear implicit and nonlinear and linear explicit monotone Fluctuation Splitting (FS) schemes (Abgrall and Mezine, 2003; Csík et al., 2002; Hubbard and Roe, 2000; Ricchiuto et al., 2005) have been implemented for the solution of Eq. (13). The numerical schemes are first order or second order accurate in time and space and obey strict mathematical design principles. These are conservation, positivity and monotonicity. Moreover, the nonlinear explicit second order scheme is linear preserving (second order accuracy at smooth solutions and first order near discontinuities).

The schemes showed to be less sensitive to spurious oscillations in shallow water applications then the original non-monotone schemes in the former version of the WWM. The source terms can be integrated within the advection part in geographical space, according to Patankar (1980) where the nonlinear contributions are linearized, or computed within a separate fractional step, using an adaptive integration technique as suggested by, e.g., Tolman (2002) for the WWIII. Beside the changes of the numerical scheme, the model abilities have been enhanced to account for varying water levels and currents fields. A detailed description of the numerical schemes, their verification and their implementation details are given by Roland (2009). In this study, the first order implicit schemes have been used for the advection part in geographical space and the nonlinear source terms have been linearized according to Patankar (1980).

The WWM was successfully applied in several studies, e.g. at the South Chinese Sea around Taiwan (Hsu et al., 2005a,b, 2006), the Baltic Sea, the U.S. East Coast including the Gulf of Mexico (Roland et al., 2005, 2006a) and for the Haringvliet estuary (Roland et al., 2006b; Zanke et al., 2006).

The new version of the WWM was verified in Roland (2009) for laboratory experiments, analytical solutions, and field observations with good results using the alternative numerical schemes of the WWM II. The source code of the new version of the WWM will be available in the near future as a free source code and will be distributed within the SHYFEM software and as a stand-alone version.

2.3. The coupling procedure

The coupling of the wave and the current models is realized using the wave induced surface stresses computed with the aid of the radiation stress theory of Longuet-Higgins and Stewart (1964). Wave transformation in shallow water areas produces a net momentum of flux also known as the “radiation stress”. The wave-induced surface stresses (gradient of the radiation stresses) in the x and y directions have been estimated in a linear form, accounting for the mean flow momentum as given in Mastenbroek et al. (1993):

$$F_x = -\frac{\partial S_{xx}}{\partial x} - \frac{\partial S_{xy}}{\partial y} \tag{14}$$

$$F_y = -\frac{\partial S_{yx}}{\partial x} - \frac{\partial S_{yy}}{\partial y} \tag{15}$$

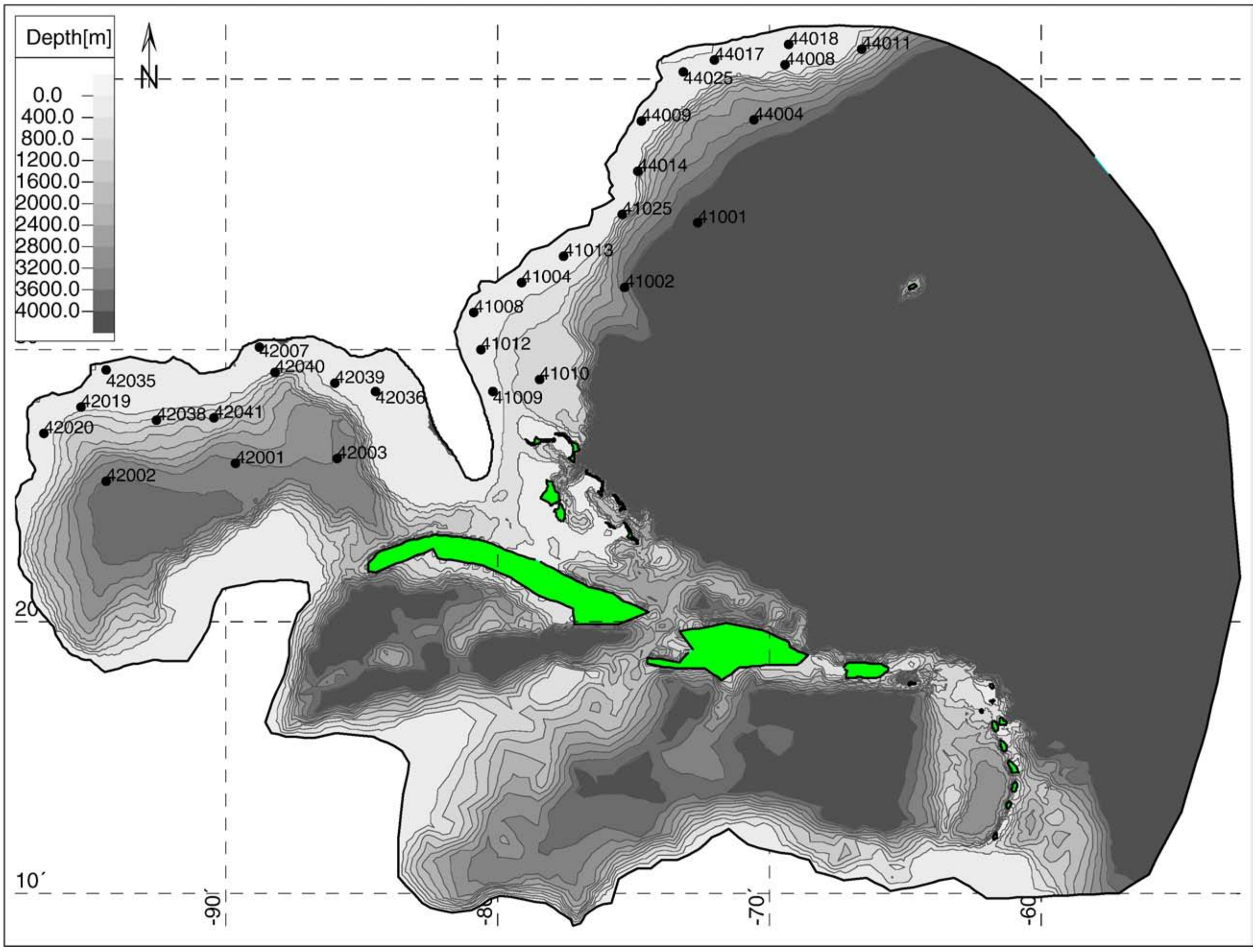

Fig. 1. Bathymetry of the U.S. East Coast and the Gulf of Mexico domain including the position of the NDBC data buoys (green circles) used for model verification. Islands are shown in green. (For interpretation of the references to colour in this figure legend, the reader is referred to the web version of this article.)

with S_{ii} being the components of the radiation stress tensor defined for a wave spectrum according to Battjes (1972) as:

$$S_{xy} = \int_0^\infty \int_{-\pi}^{\pi} N_{(\sigma,\theta)} \cdot \sigma \cdot \frac{c_{g(\sigma)}}{c_{(\sigma)}} \sin(\theta)\cos(\theta) d\theta d\sigma \tag{16}$$

$$S_{xx} = \int_0^\infty \int_{-\pi}^{\pi} N_{(\sigma,\theta)} \cdot \sigma \cdot \left[\frac{c_{g(\sigma)}}{c_{(\sigma)}}\left(\cos^2(\theta) + 1\right) - \frac{1}{2}\right] d\theta d\sigma \tag{17}$$

$$S_{yy} = \int_0^\infty \int_{-\pi}^{\pi} N_{(\sigma,\theta)} \cdot \sigma \cdot \left[\frac{c_{g(\sigma)}}{c_{(\sigma)}}\left(\sin^2(\theta) + 1\right) - \frac{1}{2}\right] d\theta d\sigma \tag{18}$$

The gradients of the radiation stresses in geographical space given in Eqs. (14) and (15) are calculated in the wave model on the foundation of linear FEM shape functions. The wave induced surface stresses are passed to the hydrodynamic model, where on the foundation of the updated boundary forcing, the new current and water level distributions are computed. Then the new hydrodynamics are passed back to the wave model where the advection velocities in the different phase spaces, Eq. (6) through Eq. (8), are recalculated using the new values of the current velocities and water levels. Finally, the WAE is solved, which closes the coupling cycle between the two models.

The communication between the SHYFEM model and the WWM is based on FIFO (First In First Out) files. These are special files in UNIX/LINUX systems, which allow two processes to communicate with each other during the runtime of each source code. The advantage of using FIFO files is that both processes are automatically synchronized when each of the processes writes/reads to the FIFO file. The data are not written to the file system, but are passed internally over the kernel of the operating system to the calling process using the system memory (see e.g., Goldt et al., 1995). The use of FIFO files for the data exchange provides both models with a universal interface to any other wave/current model. The FIFO file concept is also available under Dos/Windows type machines but it is not considered here.

3. Application and verification of the coupled model

The capability of the coupled model to simulate the wave and wind induced hydrodynamics generated by extreme meteorological events was evaluated for two different test cases. In particular, the Hurricane Ivan event, which occurred in 2004 in the Gulf of Mexico and the century storm event, which occurred in 1966 in the Northern Adriatic Sea, have been considered here. In a preceding study, the coupled current–wave model has already been applied to the Venice Lagoon in a study focused on the lagoon sediment dynamics (Ferrarin et al., 2008).

3.1. Simulation of the storm surge in the Gulf of Mexico during Hurricane Ivan

Hurricane Ivan was one of the most powerful hurricanes recorded in history. The hurricane make landfall at the Gulf Coast of Alabama in

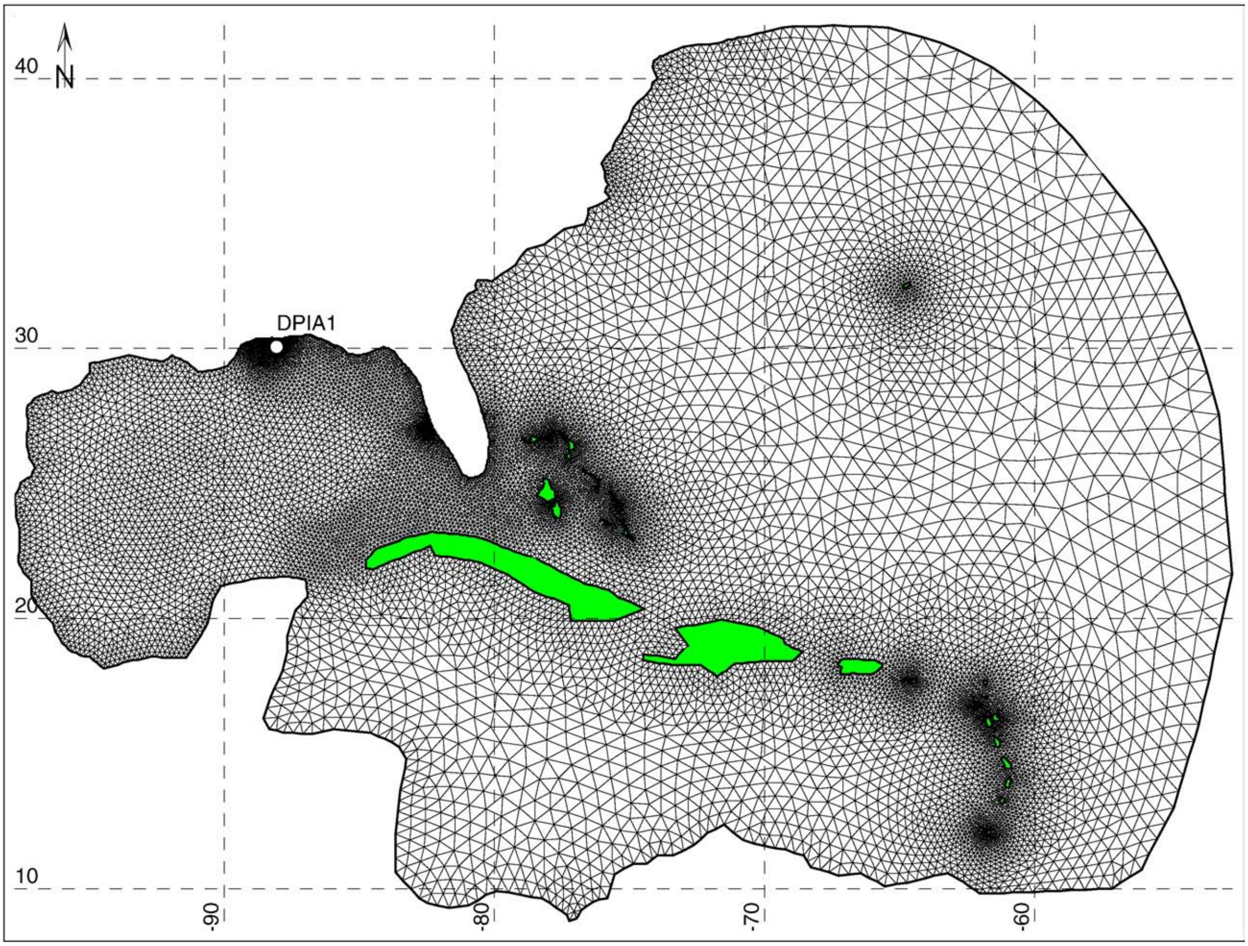

Fig. 2. Computational mesh for the U.S. East Coast and the Gulf of Mexico. DPIA1 refers to the tidal gauge at Dauphin Island.

September 2004. Ivan was a category 5 hurricane on the Saffir–Simpson scale and caused major damage to the Caribbean and the United States coasts. In order to simulate the wind and wave induced storm surge during the passage of the hurricane, the coupled model was set up on an unstructured mesh with a resolution in geographical space ranging from 0.5° in deep waters to 0.01° in the vicinity of Dauphin Island.

The atmospheric boundary conditions have been obtained from the GM (Global Model, Majewski et al., 2002) of the German Meteorological Service (DWD). The GM uses an unstructured mesh with an average resolution of 40 km. The wind fields are available every 3 h. Analyzed wind fields have been used for the simulation of the September period in the year 2004. The coupled model domain, the bathymetry and the unstructured mesh are shown in Figs. 1 and 2 respectively.

The coupled model was forced only by the surface winds from the atmospheric model. The atmospheric pressure and the contribution of the astronomical tide were neglected. The integration time step was set for the current model to 100 s and the wave model was integrated with a global time step of 300 s. For the resolution in spectral space, 36 directional bins and a relative frequency resolution $\Delta\sigma/\sigma$ of approximately 1.1 were used within a frequency range varying between 0.04 Hz and 1.00 Hz resulting in 34 frequency bins.

Verification of the wave model results have been carried out by comparison to hourly wave spectra measured by 27 NDBC buoys (National Data Buoy Center). The locations of the buoys are plotted in Fig. 2. The significant wave height (H_s) and the zero-crossing period ($Tm02$) have been estimated using the spectral moments of the measured wave spectra. The frequency bandwidth, which can be measured by the NDBC disc buoys, is limited by a maximum cut-off frequency. For most of the NDBC buoys this is 0.4 Hz. In order to obtain an appropriate comparison between the simulated and measured integral wave parameters, the spectral moments of the computed wave spectra have been recalculated using the cut-off frequency of the buoys. Table 1 summarizes the statistical results for H_s and $Tm02$ as an average for all buoys over the investigated period.

The model results compare reasonably well to the measurements and show the applicability of the wave model for the investigation area. The computed water levels estimated with the coupled model have been compared to water level measurements at Dauphin Island (30°14′54″ N 88°04′24″ W). Water level measurements are obtained with sampling periods of 6 min from the NDBC database (Station: DPIA1, see Fig. 2 for its location) for the investigated time period. In order to analyze the contribution of the wind- and wave induced

Table 1
Statistical results for the comparison of all buoys with the results of WWM II using the NEDWAM source term formulation.

	Hs	Tm02
MEAN_O	1.54	5.84
MEAN_S	1.39	5.06
BIAS	−0.15	−0.78
SCI	0.30	0.23
RMS	0.45	1.34
R^2	0.93	0.65

MEAN_O (mean of the observations), MEAN_S (mean of the simulations), BIAS (difference between mean of the observations and simulations), SCI (scatter Index), RMS (root mean square error) and R^2 (correlation coefficient).

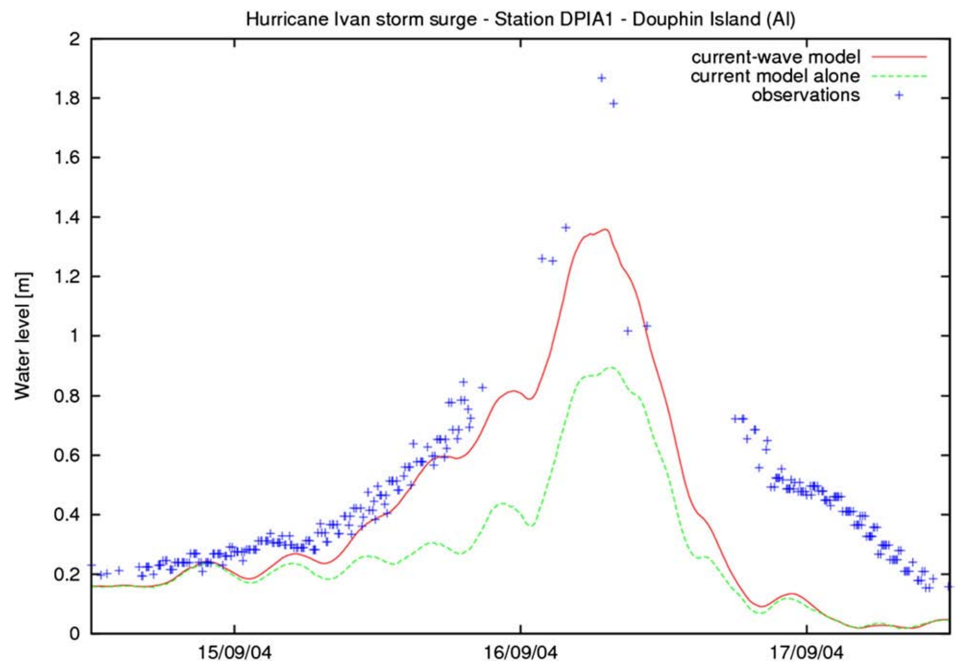

Fig. 3. Measured and hindcasted water level elevation at Dauphin Island during Hurricane Ivan.

water level elevations the differences between measured water level and the astronomical tide have been computed and compared with the model results (Fig. 3). The hydrodynamic model was run with and without wave forcing. The comparison of the resulting water level elevation at the measurement location showed clearly the strong effect of the waves on the water levels elevations during the storm surge.

The wind and wave induced rising of the water level are hindcasted well. The measured water levels are only slightly underestimated during this period. The maximum water level is underestimated by approximately 40 cm and after the storm surge, the water level is continuously underestimated. The relatively good performance of the model in this complicated situation without a rigorous tuning of the parameterizations of the model's closure terms reveals the effectivity of the coupled model. Further verification of the model is necessary, including sensitivity analysis of the wind data and the inclusion of the atmospheric pressure for this case. In terms of statistical parameters the inclusion of the wave induced water level setup reduced the root mean square error from 0.13 to 0.11 m and increased the correlation coefficient from $R = 0.75$ to 0.79.

3.2. Simulation of the 1966 storm event in the Adriatic Sea and the Venice Lagoon

The Venice Lagoon is situated at the Northwest end of the Adriatic Sea. It covers roughly an area of 500 km^2, with a major axis in the Northeast–Southwest direction, and has a length of 50 km and a width of 10 km. A complicated network of channels and shallow water flats characterizes the lagoon. A few main deep channels (maximum depth around 15 m) cross regions of otherwise very shallow water where the average water depth is about one meter. Three inlets, situated at the eastern boundary of the lagoon, allow water exchange between the northern Adriatic Sea and the lagoon. These inlets are called, from North to South, Lido, Malamocco and Chioggia and are from 500 to 1000 m wide and up to 15 m deep.

The computational domain reproduces the Adriatic Sea and the Venice Lagoon with a resolution varying from 30 m for the smallest channels of the lagoon to 30 km for the inner areas of the central Adriatic Sea. The grid consists of 15619 nodes and 28827 triangular elements (Fig. 4) with an open boundary located along the Strait of Otranto (southern grid border).

The SHYFEM hydrodynamic model has already been validated and calibrated for the Adriatic Sea–Venice Lagoon system in previous studies (Cucco and Umgiesser, 2005; Bellafiore et al., 2008). The model reproduces with good accuracy the tidal wave propagation inside the lagoon, the wind set-up, and the water exchange dynamics through the three inlets. Moreover, the coupled current–wave model was validated by comparing the simulation results against water level and wave height in different stations inside the lagoon (Ferrarin et al., 2008).

In this study, two different model applications have been carried out. In the first application, the coupled model has been applied for the year 2004 in order to validate the model for the Northern Adriatic Sea. Thereafter, in the second application, the validated model has been applied to reproduce the effect of the November 1966 storm event. In both applications, 24 frequencies, ranging from 0.2 to 1.8 Hz, and 24 uniformly distributed directions have been considered in the wind wave model and no wave conditions were prescribed at the Otranto boundary. The simulations have been carried out for one whole year using an integration time step of 300 s and 100 s for the wave model and current model respectively.

In both the 2004 and 1966 simulations, the coupled model was forced with ECMWF wind and pressure field as upper boundary conditions and with the astronomical tide as open boundary condition imposed at the southern part of the Adriatic Sea along the Strait of Otranto. Correction factors for the ECMWF wind speed were adopted as suggested by Cavaleri and Bertotti (1997). The original correction was derived according to the quality of the results available at that time. Following the progressive improvements of the ECMWF meteorological model, the correction factors have been updated continuously in time. In particular, for the November 1966 storm, the model surface boundary was forced with ECMWF global reanalysis data according to Malguzzi et al. (2006) modified with the correction factor as described above.

Measured data of significant wave heights are available at the oceanographic tower *Acqua Alta* (Cavaleri, 2000), located 15 km off the coast of the Venice Lagoon (marked with a star in Fig. 4), and have been used for model validation.

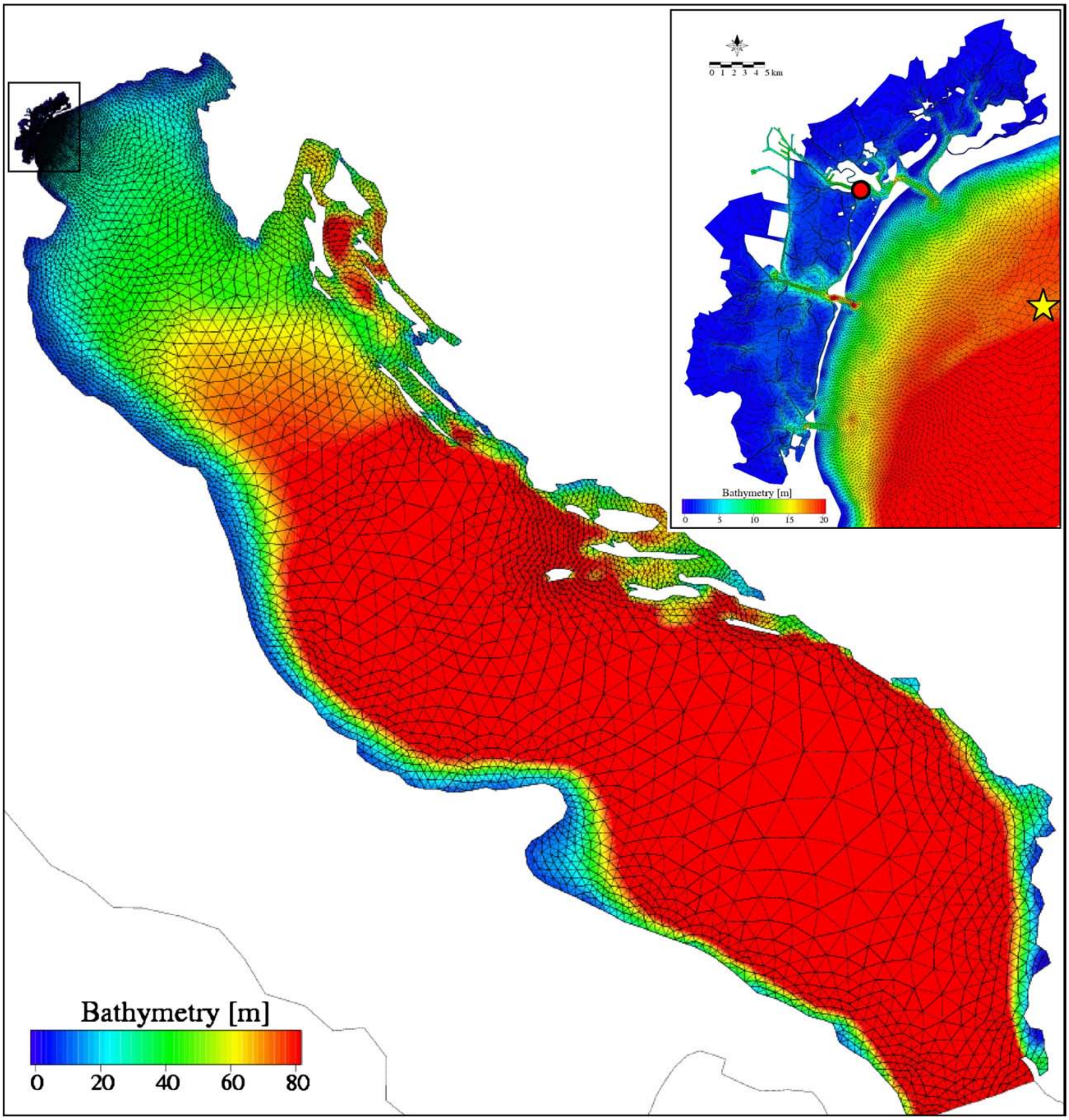

Fig. 4. Numerical grid and bathymetry of the Adriatic-Sea and Venice Lagoon system. The circle in the upper square marks the Punta Salute tidal gauge in the city of Venice and the star marks the location of the oceanographic tower "*Acqua Alta*", 15 km off the coast of the Venice Lagoon.

In Fig. 5, the model results of significant wave height are compared with observations for the whole of January 2004. The *RMS* error for the simulated period is about 0.2 m with a correlation coefficient of 0.9, revealing a satisfactory accuracy in reproducing the wind wave dynamics in the study area.

In the second stage, the coupled model has been used to reproduce the century storm of the November 1966. In the period from 3 to 5 November 1996, central and northeastern Italy was affected by a synoptic scale, severe cyclonic system that caused catastrophic and widespread damages associated with flooding, storm surges and landslides. One of the most memorable effects was the extreme high water in Venice, which reached the highest ever-recorded value of 194 cm. The southeasterly wind (Sirocco) over the Adriatic, which forced the sea level surge, has to be considered as one of the most relevant atmospheric features characterizing such an extreme meteorological event.

The computed wave field over the Adriatic Sea at 11.04.1966 at 12:00 h is shown in Fig. 6. The modelled significant wave height reaches 7 meters in front of the Venice Lagoon. No wave measurements were available at that time, but such results appear realistic considering the storm damages in the Lido and Pellestrina barrier islands.

The hydrodynamic model alone already reproduces the water level in Venice during the storm peak with good accuracy (dashed green line in Fig. 7). The influence of the waves on the water level is small near the Punta Salute station since the waves there are mainly affected by the local wind waves. The wave penetration through the inlets is not intense and only slightly influences the water levels in the central part of the lagoon. In particular, the analysis of the storm surge results without

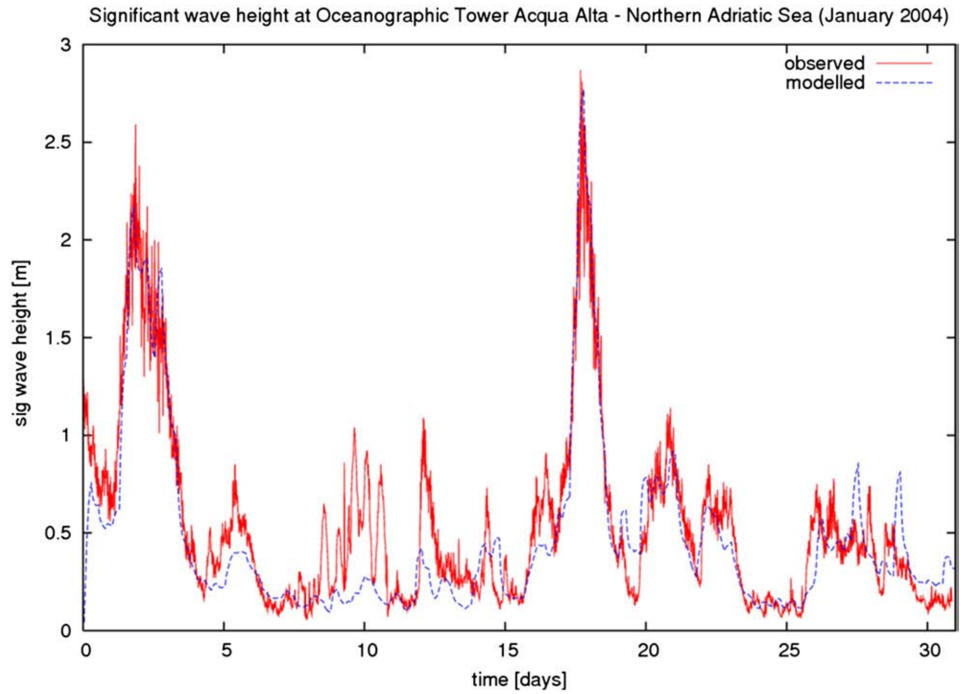

Fig. 5. Modelled and observed significant wave heights at the CNR platform, in front of the Venice Lagoon, for the period of January 2004 (see Fig. 4 for its position).

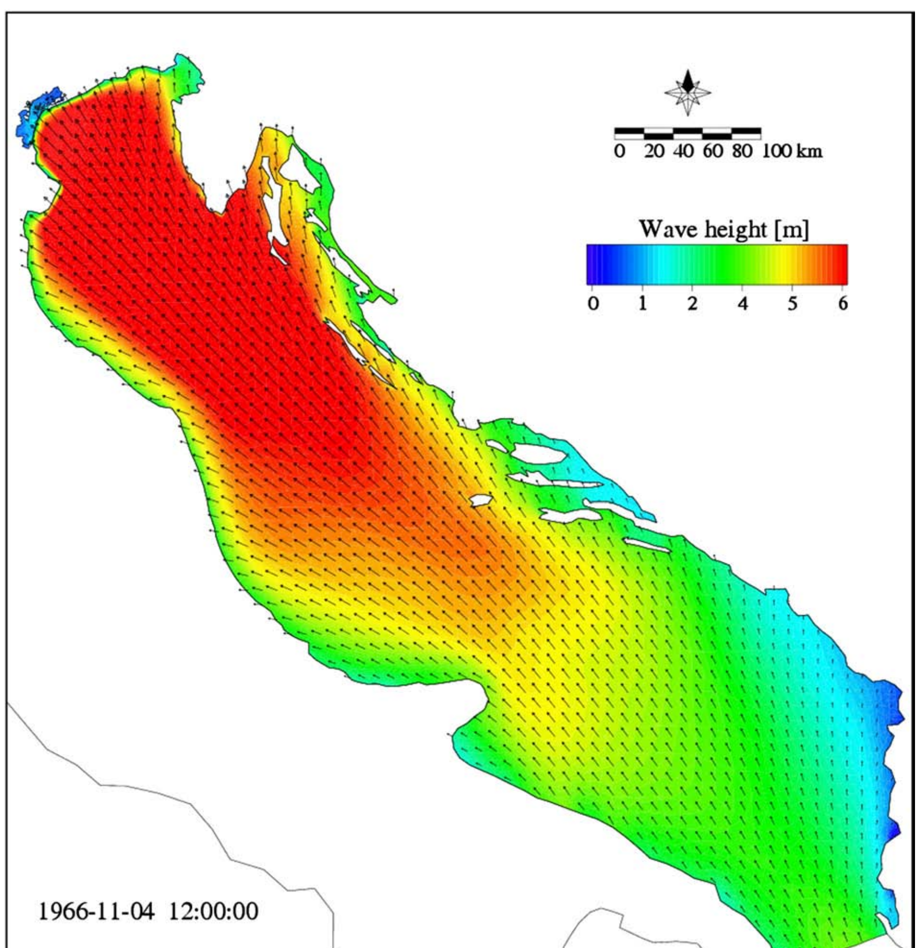

Fig. 6. Modelled significant wave height in the Adriatic Sea during the 1966 storm (The arrows indicate the mean wave direction with the arrow length scaled according to the total wave energy).

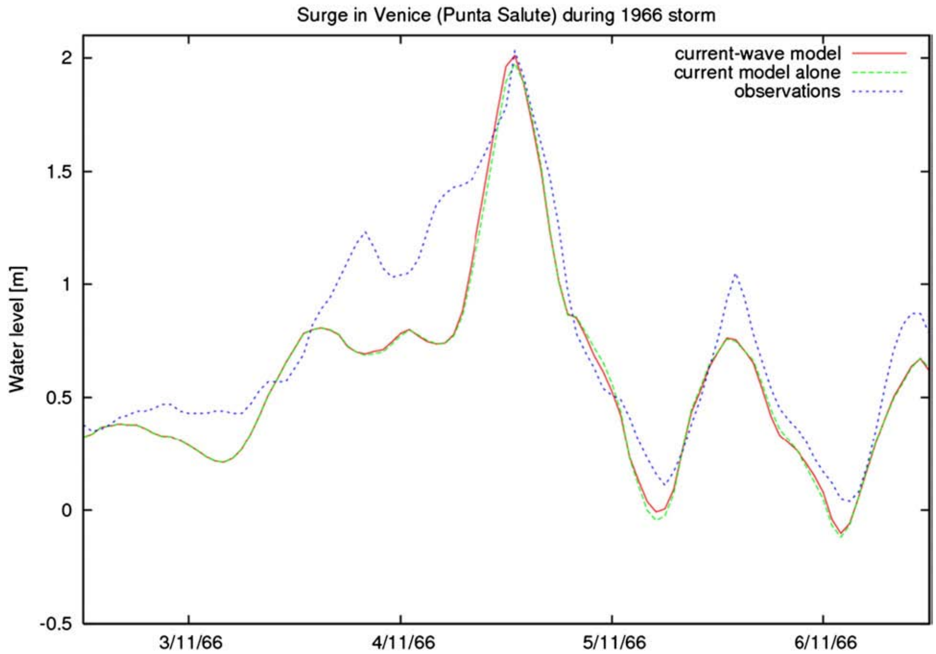

Fig. 7. Surge in Venice (Punta Salute) during 1966 storm. The continuous red line represents the storm surge modelled by the coupled current–wave model. The green dashed line represents the storm surge computed by the stand alone hydrodynamic model. The blue dotted line represents the observed storm surge. (For interpretation of the references to colour in this figure legend, the reader is referred to the web version of this article.)

wave influence reveals that the coupled model slightly improves the estimation of the storm surge peak at the "Punta Salute" station with respect to the hydrodynamic model alone (solid red line in Fig. 7).

As alluded to before, in order to investigate the effects of wind wave setup on the total water level elevation further, a simulation has been carried out in which the hydrodynamic model has been forced with the same meteorological data without the effect of the waves. Relevant differences in the water levels between the current–wave coupled model and the hydrodynamic model alone are evident especially along the barrier islands, where wave breaking is more intense (Fig. 8). In particular, water levels of about 2.2 m have been computed in front of the Lido and Pellestrina barrier islands. Such values are in line with the intensity of the flooding event that occurred in those areas, which led to the breaking of the local front sea defences. The difference plots show that the wave set-up also affects to a considerable extent the water levels inside the lagoon in some locations, especially along the border of the central basin near the Lido inlet (Fig. 8, C).

4. Discussion and outlook

The coupled wave–current model has been applied to two different real cases, a hurricane event occurring in the Gulf of Mexico and the wind, tide and wave induced water circulation in the Northern Adriatic Sea. The results for the wave heights and the water levels show good agreement with the measurement data. However, for Hurricane Ivan there is a considerable underestimation during the peak water level of the storm surge whose reason could be the coarse resolution of the wind data and the neglect of the atmospheric pressure in the computations.

The application of the coupled model to the Adriatic Sea and the Venice Lagoon showed that at the measurement location "Punta Salute", the influence of the waves on the water levels is small. The reason for this is the sheltering effects of the barrier island, which protects the inner part of the lagoon from the open sea waves' impact. Nevertheless, the results show the importance of the wave–current interaction in simulating the intense water levels set-up occurring outside the lagoon basin in front of the barrier islands.

Already in the actual version of the source the coupled model needed only approx. 60 s computational time, on a modern computer (Athlon64® X2 6000+) platform using one CPU core, to calculate one coupling cycle (300 s real-time) for the Hurricane Ivan scenario. The performance analysis of the coupled model showed that the wave model is the bottleneck of the coupled model and that it needs further improvement, e.g. the effective parallelization of the model code. This will be done using the domain decomposition technique, e.g. with the aid of the METIS library (Karypis and Kumar, 1999).

The new coupled model can efficiently be used in complicated coastal environments for various applications where both waves and currents are of importance and their interaction cannot be neglected. Moreover, it provides the research community with a numerical platform, which can be used efficiently for further developments with respect to the formulation of the source terms given by, e.g., Babanin et al. (2007) or Ardhuin et al. (2008b).

More sophisticated wave–current coupling theories as suggested, e.g., by Smith (2006) for the vertical integrated momentum equations or by Ardhuin et al. (2008a) for a fully 3d-treatment of the wave momentum will be implemented in the future. The coupled model is freely available, relatively easy to use and setup. We feel that it can be effectively used, e.g., for manoeuvre planning and rapid environmental assessment in complicated costal environments, where the influence of the waves on the currents and vice versa cannot be neglected.

5. Conclusions

A fully coupled, freely-available, wave–current model, which can handle unstructured triangular meshes, was presented in this paper. The spectral 3rd generation wave model WWM II was coupled with SHYFEM. The suggested coupling procedure between the wave and the current model, as well as the numerical schemes of both models have been successfully tested and showed to be effective for simulating wind and wave induced storm surges during investigated extreme events. The coupling approach using FIFO pipes allows the two processes to communicate over the system memory without the need of writing the data to hard disk, which slows down the model performance. The source code of the coupled model can be obtained from any of the authors.

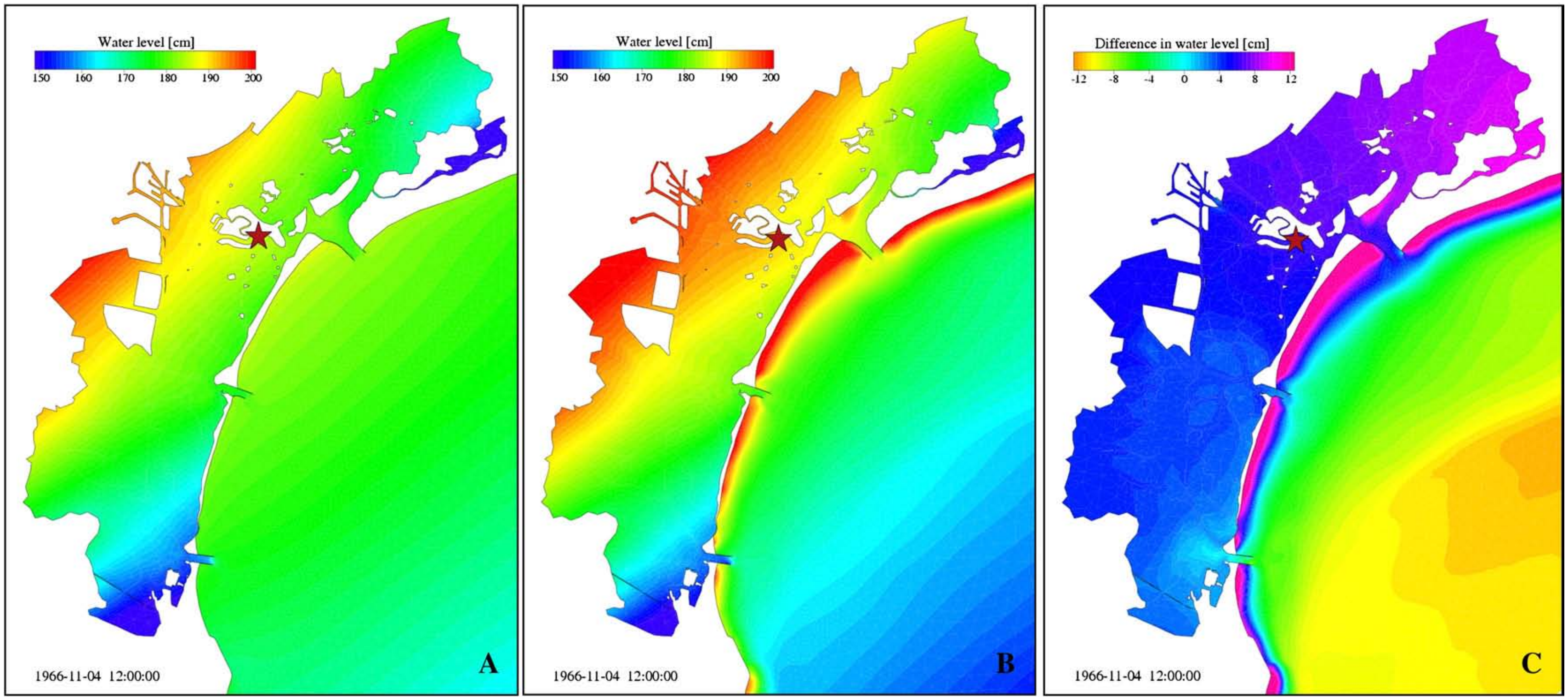

Fig. 8. Water level distribution during 1966 storm. A) Hydrodynamic model stand-alone; B) coupled current–wave model; C) difference in water level between B and A. The red star indicates the Punta Saluta tidal station. (For interpretation of the references to colour in this figure legend, the reader is referred to the web version of this article.)

Acknowledgments

The authors wish to thank Luigi Cavaleri and Luciana Bertotti for providing wind data of the Adriatic storm surge of November 1966. Moreover, we like to thank the unknown reviewers for the constructive and helpful comments and recommendations.

References

Abgrall, R., Mezine, M., 2003. Construction of second order accurate monotone and stable residual distribution schemes for unsteady flow problems. J. Comput. Phys. 188, 16–55.
Alves, J.H.G.M., Greenslade, D.J.M., Banner, M.L., 2002. Impact of a saturation-dependent dissipation source function on operational hindcasts of wind–waves in the Australian Region. J. Atmos. Ocean Sci. 8 (4), 239–267.
Ardhuin, F., Herbers, T.H.C., van Vledder, G.P., Watts, K.P., Jensen, R., Graber, H.C., 2007. Swell and slanting-fetch effects on wind wave growth. J. Phys. Oceanogr. 37, 908–931.
Ardhuin, F., Rascle, N., Belibassakis, K.A., 2008a. Explicit wave-averaged primitive equations using a generalized lagrangian mean. Ocean Model. 20, 35–60.
Ardhuin, F., Collard, F., Chapron, B., Queffeulou, P., Filipot, J.-F., Hamon, M., 2008b. Spectral wave dissipation based on observations: a global validation. Chinese–German Joint Symposium on Hydraulic and Ocean Engineering, Darmstadt, Germany.
Babanin, A., Tsagareli, K., Young, I., Walker, D., 2007. Implementation of new experimental input/dissipation terms for modelling spectral evolution of wind waves. 10th International Workshop on Wave Hindcasting and Forecasting, North Shore, Oahu, Hawaii.
Battjes, J.A., 1972. Radiation stresses in short-crested waves. J. Mar. Res. 30, 56–64.
Battjes, J.A., Janssen, J.P.F.M., 1978. Energy loss and set-up due to breaking of random waves. Proc. 16th Int. Conf. Coastal Engineering, ASCE, pp. 569–587.
Bellafiore, D., Umgiesser, G., Cucco, A., 2008. Modelling the water exchange between the Venice Lagoon and the Adriatic Sea. Ocean Dynamics. WWW Page, http://www.springerlink.com/content/6457522363787750/fulltext.pdf. doi:10.1007/s10236-008-0152-7.
Bouws, E., Komen, G.J., 1983. On the balance between growth and dissipation in an extreme depth-limited wind–sea in the southern North Sea. J. Phys. Oceanogr. 13, 1653–1658.
Cavaleri, L., 2000. The oceanographic tower Acqua Alta — activity and prediction of sea states at Venice. Coast. Eng. 39 (1), 29–70.
Cavaleri, L., Bertotti, L., 1997. In search of the correct wind and wave fields in a minor basin. Mon. Weather Rev. 125 (8), 1964–1975.
Cucco, A., Umgiesser, G., 2005. Modeling the Venice Lagoon residence time. Ecol. Model. 193 (1–2), 34–51.
Csík, Á., Ricchiuto, M., Deconinck, H., 2002. A conservative formulation of the multidimensional upwind residual distribution schemes for general non linear conservation laws. J. Comput. Phys. 179 (1), 286–312.
Donea, J., 1984. A Taylor–Galerkin Method for Convective Transport Problem. Int. J. Numer. Methods Eng. 20, 101–119.
Eldeberky, Y., 1996. Nonlinear Transformation of Wave Spectra in the Nearshore Zone, Ph.D. Thesis, TU-Deft, The Netherlands.
Ferrarin, C., Umgiesser, G., 2005. Hydrodynamic modeling of a coastal lagoon: the Cabras lagoon in Sardinia, Italy. Ecol. Model. 188, 340–357.
Ferrarin, C., Umgiesser, G., Cucco, A., Hsu, T.-W., Roland, A., Amos, C.L., 2008. Development and validation of a finite element morphological model for shallow water basins. Coast. Eng. 55 (9), 716–731.
Goldt, S., van der Meer, S., Burkett, S., Welsh, M., 1995. The Linux Programmer's Guide. WWW Page, http://tldp.org/LDP/lpg/.
Günther, H., Hasselmann, S., Janssen, P., 1992. The WAM model Cycle 4 (revised version). Dtsch. Klim. Rechenzentrum, Tech. Rep. 4.
Hasselmann, K., 1962. On the non-linear energy transfer in a gravity wave spectrum, part 1: general theory. J. Fluid Mech. 12, 481–501.
Hasselmann, S., Hasselmann, K., 1985. Computations and parameterizations of the nonlinear energy transfer in a gravity–wave spectrum. Part I: A new method for efficient computations of the exact nonlinear transfer integral. J. Phys. Oceanogr. 15 (1), 369–377.
Hasselmann, K., Barnett, T.P., Bouws, H., Carlson, H., Cartright, D.E., Enke, K., Ewing, J.A., Gineapp, H., Hasselmann, D.E., Kruseman, P., Meerburg, A., Muller, P., Olbers, D.J., Richter, K., Sell, W., Walden, H., 1973. Measurements of wind wave growth and swell decay during the Joint North Sea Wave Project (JONSWAP). Dtsch. Hydrogr. Z., Suppl. 12, A8.
Hashimoto, N., Kawaguchi, K., 2001. Extension and modification of Discrete Interaction Approximation (DIA) for computing nonlinear energytransfer of gravity wave spectrum. Ocean Wave Measurement and Analysis. ASCE, New York, pp. 530–539.
Hubbard, M.E., Roe, P.L., 2000. Compact high-resolution algorithms for time-dependent advection on unstructured grids. Int. J. Numer. Methods Fluids 33, 711–736.
Hsu, T.-W., Ou, S.-H., Liau, J.-M., 2005a. Hindcasting near shore wind waves using a FEM code for SWAN. Coast. Eng. 52, 177–195.
Hsu, T.-W., Ou, S.-H., Liau, J.-M., Zanke, U., Roland, A., Mewis, P., 2005b. Development and implement of a spectral finite element wave model, Waves 2005, ASCE/COPRI. The Fifth International Symposium on Wave Measurement and Analysis. Ed. Billy Edge, Madrid, Spain.
Hsu, T.-W., Ou, S.-H., Liau, J.-M., Lin, J.-G., Kao, C.-C., Roland, A., Zanke, U., Shin, C.-Y., 2006. Application of data assimilation for spectral wave model on unstructured meshes. The 25th International Conference on Offshore Mechanics and Arctic Engineering, Hamburg, Germany.
Karypis, G., Kumar, V., 1999. A fast and high quality multilevel scheme for partitioning irregular graphs. SIAM J. Sci. Comput. 20 (1), 359–392.
Komen, G.J., Hasselmann, K., Hasselmann, S., 1984. On the existence of a fully developed wind sea spectrum. J. Phys. Oceanogr. 14, 1271–1285.
Kudryavtsev, V.N., Makin, V.K., Chapron, B., 1999. Coupled sea surface–atmosphere model 2. Spectrum of short wind waves. J. Geophys. Res. 104, 7625–7639.
Leonard, B.P., 1991. The ULTIMATE conservative difference scheme applied to unsteady one-dimensional advection. Comput. Methods Appl. Mech. Eng. 88, 17–74.
Longuet-Higgins, M.S., Stewart, R.W., 1964. Radiation stresses in water waves; A physical discussion with applications. Deep-Sea Res. 11, 529–562.
Makin, V.K., Kudryavtsev, V.N., 1999. Coupled sea surface- atmosphere model 1. Wind over waves coupling. J. Geophys. Res. 104, 7613–7623.
Makin, V.K., Stam, M., 2003. New drag formulation in NEDWAM. KNMI, Technical Report: TR-250. De Bilt, The Netherlands. WWW Page, www.knmi.nl/publications/fulltexts/makinstam.pdf.
Malguzzi, P., Grossi, G., Buzzi, A., Ranzi, R., Buizza, R., 2006. The 1966 "century" flood in Italy: a meteorological and hydrological revisitation. J. Geophys. Res. 111. doi:10.1029/2006JD007111.
Mastenbroek, C., Burgers, G., Janssen, P., 1993. The dynamical coupling of a wave model and a storm surge model through the atmospheric boundary layer. J. Phys. Oceanogr. 23, 1856–1867.
Majewski, D., Frank, H., Liermann, D., Ritter, B., 2002. Kurze Beschreibung des Global-Modells GME (40 km/L 40) und seiner Datenbanken auf dem Datenserver (DAS3/4) des DWD, German Weather Service (DWD). Offenbach, Germany.
NDBC (National Data Buoy Center), WWW Page, http://www.ndbc.noaa.gov/hmd.shtml.
Patankar, S., 1980. Numerical Heat Transfer and Fluid Flow. McGraw-Hill.
Rasmussen, H., 1998. Stochastic and Deterministic Modelling of Surface Gravity Waves in Finite Depth, PhD Thesis, Technical University of Denmark (DTU), Institute for Hydrodynamics and Hydraulic Engineering.
Ricchiuto, M., Csík, Á., Deconinck, H., 2005. Residual distribution for general time-dependent conservation laws. J. Comput. Phys. 209 (1), 249–289.
Roland, A., 2009. Development of WWM II — Spectral wave modelling on unstructured meshes, PhD Thesis, Darmstadt University of Technology, Institute for Hydraulic Engineering and Water Resources Management, Darmstadt, Germany.
Roland, A., Mewis, P., Zanke, U., Ou, S.-H., Hsu, T.-W., Liau, J.-M., 2005. Verification and improvement of a spectral finite element wave model, Waves 2005, ASCE/COPRI. The Fifth International Symposium on Wave Measurement and Analysis. Ed. Billy Edge, Madrid, Spain.
Roland, A., Zanke, U., Hsu, T.-W., Ou, S.-H., Liau, J.-M., Wang, S.-K., 2006a. Verification a 3rd generation FEM spectral wave model for shallow and deep water applications. The 25th International Conference on Offshore Mechanics and Arctic Engineering, Hamburg, Germany.
Roland, A., Zanke, U., Hsu, T.-W., Ou, S.-H., Liau, J.-M., 2006b. Spectral wave modelling on unstructured grids with the WWM (Wind Wave Model) I: The deep water cases. Third Chinese–German Joint Symposium on Coastal and Ocean Engineering, Tainan, Taiwan.
Scroccaro, I., Matarrese, R., Umgiesser, G., 2004. Application of a finite element model to the Taranto Sea. Chem. Ecol. 20 (Suppl. 1), 205–224.
Selmin, V., Donea, J., Quartapelle, L., 1985. Finite element methods for nonlinear advection. Comput. Methods Appl. Mech. Eng. 52, 817–845.
Smith, J.A., 2006. Wave–current interactions in finite-depth. J. Phys. Oceanogr. 36 (7), 1403–1419.
Stiassnie, M., 2001. Nonlinear interaction of inhomogeneous random water wave. ECMWF Report of the Workshop on Ocean Waves Forecasting, Reading, U.K.
Tolman, H.L., 1995. On the selection of propagation schemes for a spectral wind–wave model. NWS/NCEP Office Note 411, NCEP/OMW, 5200 Auth Road, Camp Springs, MD 21401.
Tolman, H.L., 2002. User manual and system documentation of WAVEWATCH-III version 2.22. Technical Report 222, NOAA/NWS/NCEP/MMAB. WWW Page, http://polar.ncep.noaa.gov/waves/wavewatch/wavewatch.html.
Umgiesser, G., 1997. Modelling the Venice Lagoon. Int. J. Salt Lake Res. 6, 175–199.
Umgiesser, G., Bergamasco, A., 1995. Outline of a primitive equations finite element model. Rapporto e Studi, Istituto Veneto of Scienze, Lettere ed Arti XII, pp. 291–320.
Umgiesser, G., Melaku Canu, D., Cucco, A., Solidoro, C., 2004. A finite element model for the Venice Lagoon. Development, set up, calibration and validation. J. Mar. Syst. 51, 123–145.
van Vledder, G.Ph., 2006. The WRT method for the computation of non-linear four-wave interactions in discrete spectral wave models. Coast. Eng. 53, 223–242.
Whitham, G.B., 1974. Linear and Nonlinear Waves. Wiley, New York.
Yanenko, N.N., 1971. The Method of Fractional Steps. Springer-Verlag.
Zakharov, V.E., 1968. Stability of finite amplitude periodic waves on deep liquid surface. J. Appl. Mech. Tech. Phys. 2, 86–91.
Zanke, U., Roland, A., Hsu, T.W., Ou, S.H., Liau, J.M., 2006. Spectral wave modelling on unstructured grids with the WWM (Wind Wave Model) — II: The shallow water cases. Third Chinese–German Joint Symposium on Coastal and Ocean Engineering (JOINT2006), Tainan, Taiwan.